

The Influence of Noise in Dynamic PET Direct Reconstruction

Michele Scipioni^{1,2}, M. Filomena Santarelli^{3,2}, Vincenzo Positano² and Luigi Landini^{1,2}

¹ Department of Information Engineering, University of Pisa, Pisa, PI, Italy

² Fondazione G. Monasterio, CNR-Regione Toscana, Pisa, PI, Italy

³ Institute of Clinical Physiology, CNR, Pisa, PI, Italy

Abstract— In the present work a study is carried out in order to assess the efficiency of the direct reconstruction algorithms on noisy dynamic PET data. The study is performed via Monte Carlo simulations of a uniform cylindrical phantom whose emission values change in time according to a kinetic law. After generating the relevant projection data and properly adding the effects of different noise sources on them, the direct reconstruction and parametric estimation algorithm is applied. The resulting kinetic parameters and reconstructed images are then quantitatively evaluated with appropriate indexes. The simulation is repeated considering different sources of noise and different values of them. The results obtained allow us to affirm that the direct reconstruction algorithm tested maintains a good efficiency also in presence of noise.

Keywords— dynamic positron emission tomography, direct reconstruction, kinetic analysis, compartmental model, noise

I. INTRODUCTION

Positron emission tomography (PET) dynamic studies are performed to quantify tissue-specific biochemical properties. When acquiring a dynamic PET scan, the activity of the PET tracer is measured at multiple time points, involving a sequence of acquisitions.

In routine use PET scanners, acquired data are subject to several noise sources, such as accidental scattering, random scattering and attenuation [1]. Such unwanted events can compromise accuracy in determining the tracer behaviour if not suitably corrected or accounted for. Moreover, in digital image acquisition in addition to the stochastic nature of the photon-counting, the intrinsic thermal and electronic noise should be accounted for.

In conventional reconstruction and analysis methods the sequence of emission images is first reconstructed and then, in a separate step, the estimation of kinetic parameters from time activity curves (TACs) is performed. The kinetic parameter estimation is based on the application of a compartment model analysis; it allows to determine the pharmacokinetic behaviour of the administered drug in a target organ [2]. This process is known as kinetic analysis. Kinetic analysis in a

voxel-by-voxel fashion provides parametric images that can be used to determine the spatial distribution of the behaviour of specific tracer [3].

Recently, direct reconstruction methods have been proposed, that combine emission image reconstruction and kinetic modelling into a single formula and estimate parametric images directly from raw projections [4] or list mode data, as well [5]. The most recent direct algorithms proposed in literature are presented as "generalized algorithms", because they do not depend on a specific kinetic model. Among those generalized algorithms, the one proposed in [6] results very efficient, both in terms of computing and of kinetic parameters estimation performances. Such algorithm (called OTEM, optimization transfer with expectation-maximization surrogate) uses an expectation-maximization (EM) based surrogate function in the image domain for direct reconstruction of non-linear parametric images in dynamic PET. The EM surrogate function is maximized by using penalized maximum likelihood (ML) method, based on a modified Levenberg-Marquardt algorithm. It has been proven that OTEM algorithm can achieve a better bias-variance performance than the indirect reconstruction algorithms. Moreover, its convergence rate is substantially faster than previous direct reconstruction algorithms [6].

However, no studies have been performed so far about the evaluation of the performance of this new class of direct reconstruction algorithms, such as the OTEM algorithm, when noisy data are considered. In fact, it is well known that the presence of noise sources compromises the estimation of the emission density when ML reconstruction algorithms are used [7, 8].

In the present work we study the behaviour of this particular direct reconstruction algorithm, starting from dynamic PET data with different noise degrees. Such evaluation is performed by simulating realistic PET measured data, and analysing them via the OTEM algorithm.

II. THEORY

The concentration of the radio-tracer at a given pixel at time t can be described by the following general tracer kinetic

model [9]:

$$C_T(t, k, f_v) = (1 - f_v)h(t, k) \otimes C_p(t) + f_v C_{wb}(t) \quad (1)$$

where k is the vector of the kinetic parameters that determines the tracer uptake in the tissue, f_v is the fractional volume of blood in the tissue, $h(t, k)$ is the tissue impulse response function, $C_p(t)$ is the tracer concentration in plasma, $C_{wb}(t)$ is the tracer concentration in whole blood; \otimes is the convolution operator. The image intensity at pixel p in time frame t , $x_t(K_p)$, is then given by:

$$x_t(K_p) = \int_{t_s}^{t_e} C_T(\tau, K_p) e^{-\lambda \tau} d\tau \quad (2)$$

where the integral is evaluated between the start and end times of frame t , K_p is a vector containing the fractional volume of blood f_v and the kinetic parameters k_j ($K_p = [f_v, K_1, k_2, k_3, k_4]_p$) relative to the p^{th} pixel and λ is the decay constant of the radio-tracer. PET measured data can be modelled as a collection of independent Poisson random variables with the expected projection $\bar{y}_t(K)$ in time frame t related to the dynamic image $x_t(K)$ through an affine transform:

$$\bar{y}_t(K) = Ax_t(K) + r_t \quad (3)$$

where A is the system matrix, r_t is the expectation of scattered and random events in the t^{th} frame. In the model presented in (3), the expected measurement noise is assumed to be null (white Gaussian noise).

In order to estimate the parameters matrix K according to ML method, the following log-likelihood function of the dynamic PET data must be evaluated [6]:

$$L(y|K) = \sum_{t=1}^{T_{tot}} \sum_{i=1}^{D_{tot}} y_{it} \log \bar{y}_{it}(K) - \bar{y}_{it}(K) \quad (4)$$

where T_{tot} is the total number of time frames, D_{tot} is the total number of the detector pairs, \bar{y}_{it} is the expected measurement of detector pair i in time frame t , from (3).

Direct reconstruction finds the solution by maximizing the following penalized likelihood function:

$$\theta(K) = L(y|K) - \beta U(K) \quad (5)$$

$$\hat{K} = \underset{K}{\arg \max} \theta(K) \quad (6)$$

where $U(K)$ is a smoothness penalty and β is the regularization parameter that controls the trade-off between resolution and noise. The smoothness penalty can be applied either on the kinetic parameters K or on the dynamic image $x_t(K)$, depending on the application.

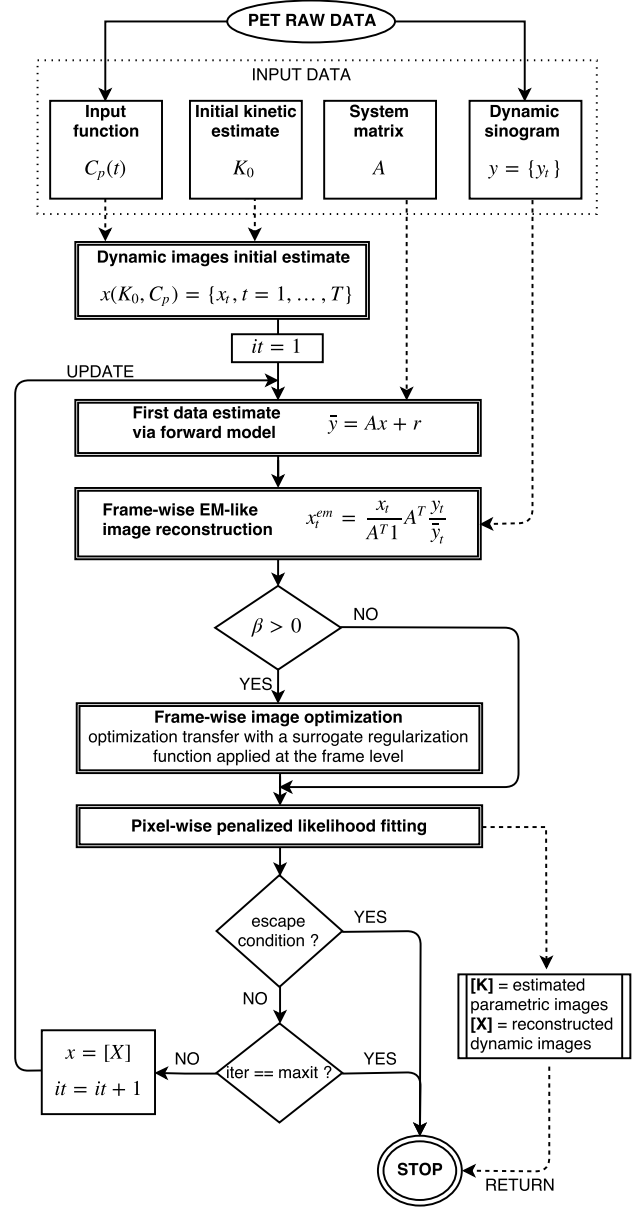


Fig. 1: Schematic flow diagram of the OTEM direct reconstruction algorithm

A. Direct reconstruction algorithm

The direct reconstruction algorithm we used is the OTEM algorithm. It performs a ML reconstruction, including a penalized likelihood function, shown in eq. 6. Such algorithm performs non linear fitting with a modified Levenberg-Marquardt method.

Details of the algorithm are described in [6]. In fig. 1 a

schematic flow diagram of the OTEM algorithm is shown. As we can see from the diagram, the output of the algorithm consists on the $n + 1$ parametric images $[K]$ (relevant to f_v and k_j parameters, $j = 1 \dots n$), and the reconstructed dynamic images $[X]$.

III. METHODS

A. Simulation

We performed Monte Carlo simulations in order to evaluate the goodness of the kinetic parameters estimation and image generation with the OTEM direct reconstruction algorithm in presence of noise.

Emission sinograms are generated by projection of two-dimensional radioactivity distribution functions into sinograms (true coincidences). On each sinogram, random and scatter coincidences, and measurement noise are added to account for theoretical and experimental evidence.

A uniform cylindrical phantom with radius of 10 cm and length of 15 cm, in a circular field of view (FOV) of 70 cm in diameter is generated; the total number of pixels on the image plane was $n_x \times n_y = 128 \times 128$. Dynamic emission data were generated changing the emission mean value inside the cylinder frame-by-frame, according to the two-tissue, 4-k parameter kinetic model [9]. The k-values used as input to the simulation are shown in table 1, where T1 tissue simulates a highly irreversible condition (typical for example in cerebral tissue) while T2 tissue simulates a more reversible condition (typical for example in liver), for ^{18}F -FDG tracer.

	f_v	K_1	k_2	k_3	k_4	K_i
T1	0.05	0.082	0.055	0.085	0.002	0.0497
T2	0.03	0.426	0.660	0.010	0.022	0.0064

Table 1: Input K-values used in the simulation. f_v is expressed as % value; units for K_1 and K_i are $\text{ml}/\text{cm}^3/\text{min}$ while for k_j ($j = 2 \dots 4$) are min^{-1} . T1 tissue simulates a highly irreversible condition (typical for example in cerebral tissue) while T2 tissue simulates a more reversible condition (typical for example in liver)

Emission time frame duration varied according to typical values used in clinical PET data acquisitions: 12 frames \times 10sec + 2 \times 30sec + 3 \times 60sec + 2 \times 120sec + 5 \times 300sec, for a total of acquisition time of 2000sec. For each emission time frame, Poisson events are generated with the mean value equal to the relevant input emission value data. Projected data (sinograms) were generated according to eq. 3; they consist of $n_b \times n_a = 186 \times 360$ points, where n_b is the number of points

for each projection and n_a is the number of angles from $-\pi$ to π .

The noisy data were generated including random scattering (RS), accidental coincidences (AC) and measurement noise (GN). AC were generated as Poisson events identically distributed in the sinogram, with a constant mean value. RS in the sinogram was modelled as a Gaussian function having its maximum at the center of each projection, and extending to the tails, which are outside the source boundary; the Gaussian function values are the means of a Poisson events generator.

In the simulation, the RS values were from 0% to 45% of the maximum value of the sinogram points and, equally, AC values were from 0% to 45%. In order to include the measurement noise (GN) a Gaussian white noise, with mean null and variance equal to 2% of the maximum sinogram value, was added on the sinogram. On each sinogram, a combination of random, accidental events (RS + AC) was added to obtain the total sinogram, together with the GN. Simulation has been repeated 50 times, for each noisy condition.

B. Figures of merit: quantifying the estimation error of kinetic parameters and reconstructed images

In order to evaluate the estimation errors due to the presence of noise, the following indexes have been computed on the produced data.

As far as the kinetic parameters estimations and the fractional blood volume, the percentage of errors is evaluated:

$$\%k_j = \frac{\hat{k}_j - k_j}{k_j}, j = 1 \dots 4 \quad (7)$$

$$\%f_v = \frac{\hat{f}_v - f_v}{f_v} \quad (8)$$

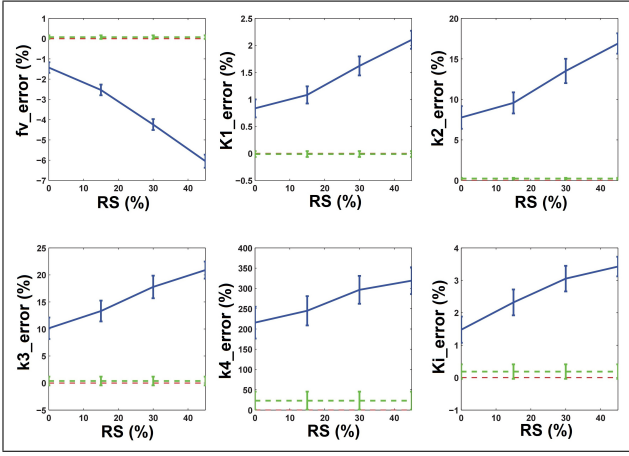
where k_j and f_v are the input parameters values used in the simulation, and \hat{k}_j and \hat{f}_v are the relevant estimated values.

The macro-parameter K_i ($K_i = \frac{K_1 k_3}{k_2 + k_3}$) is often taken into account in dynamic PET data analysis, especially in clinical studies; in the present work, the estimated K_i values are also considered, and the eq. 7 is applied on them, as well.

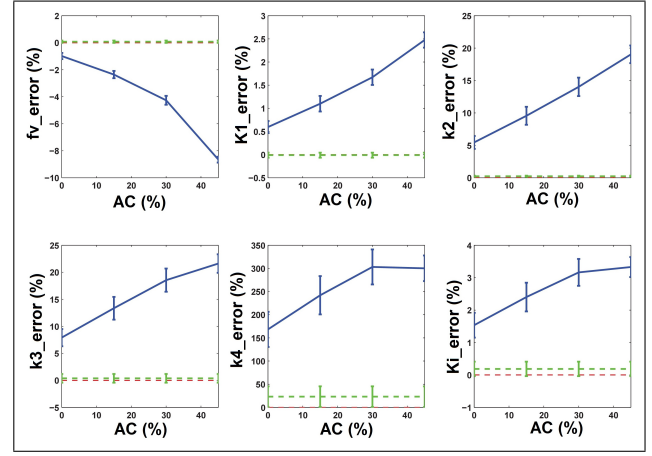
In order to evaluate the goodness of the reconstructed images, for each time frame, the following error is evaluated:

$$E \left(\frac{\hat{X}(t) - X(t)}{X(t)} \right), t = 1 \dots T_{tot} \quad (9)$$

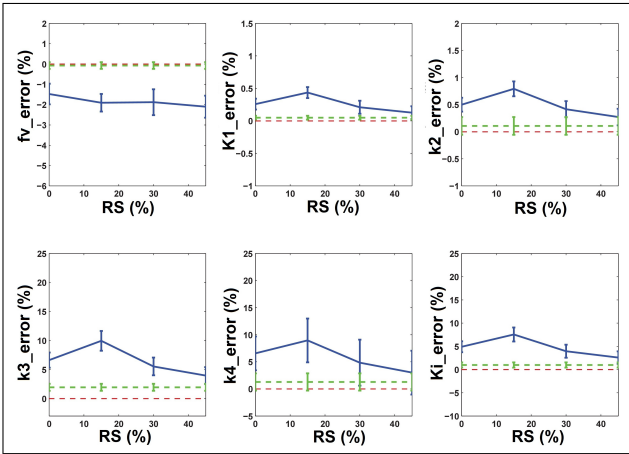
where $X(t)$ is the input image at frame time t and $\hat{X}(t)$ is the relevant reconstructed image; the E in the eq.9 represents the mean operation.



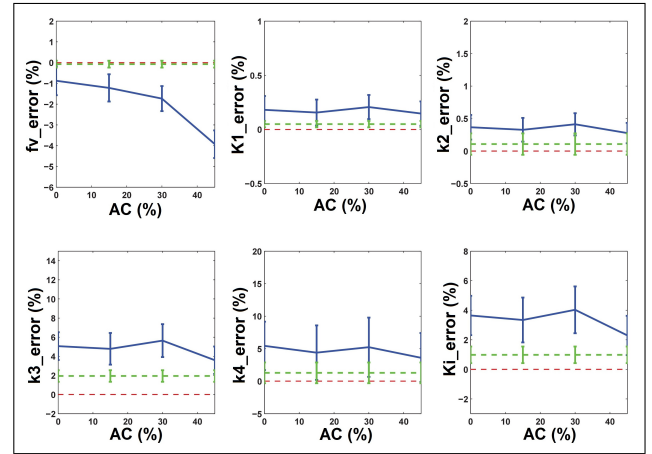
(a) Effect of randoms on T1 phantom with AC=30% and GN=2%



(b) Effect of scattering on T1 phantom with RS=30% and GN=2%



(c) Effect of randoms on T2 phantom with AC=30% and GN=2%



(d) Effect of scattering on T2 phantom with RS=30% and GN=2%

Fig. 2: Percentage errors of estimated f_v , k_j for $i = 1, \dots, 4$ and K_i evaluated according to eq.7 and eq. 8. (a) and (b) refer to tissue T1, while (c) and (d) refer to T2. Red lines represent the zero reference, while the green lines are the estimation errors of the value of the parameters on noiseless data.

IV. RESULTS

In fig.2 the percentage errors, and standard deviations, of estimated f_v , k_j , $j = 1, \dots, 4$ and the macro parameter K_i evaluated according to eq.7 and eq. 8 are shown. In the figure, red lines represent the reference of zero error, while the green lines are the estimation errors of the value of the parameters on data without noise. The results shown in (a) and (b) are relevant to the input k-values of T1 in tab.1; the results shown in (c) and (d) are relevant to the input k-values of T2 in tab.1. The results in (a) and (c) are obtained with fixed AC value at 30%, while the results shown in (b) and (d) are obtained with fixed RS = 30%; in all the figures the GN is fixed at 2%.

In fig.3 the dynamic images reconstruction errors, evalu-

ated according to eq. 9 for different noise percentages, are shown, with the relevant TACs superimposed: results in (a) are obtained from the input k-values of T1 in tab.1 and those in (b) are obtained from the input values of T2; in both the figures, the GN is fixed at 2%.

V. DISCUSSION

From the simulation results it is evident that, as expected, when the noise increases the percentage error of the parameters estimation increases. However, also the following considerations arise.

The f_v parameter estimation gives always a negative percentage error; it means that the fractional volume of blood in

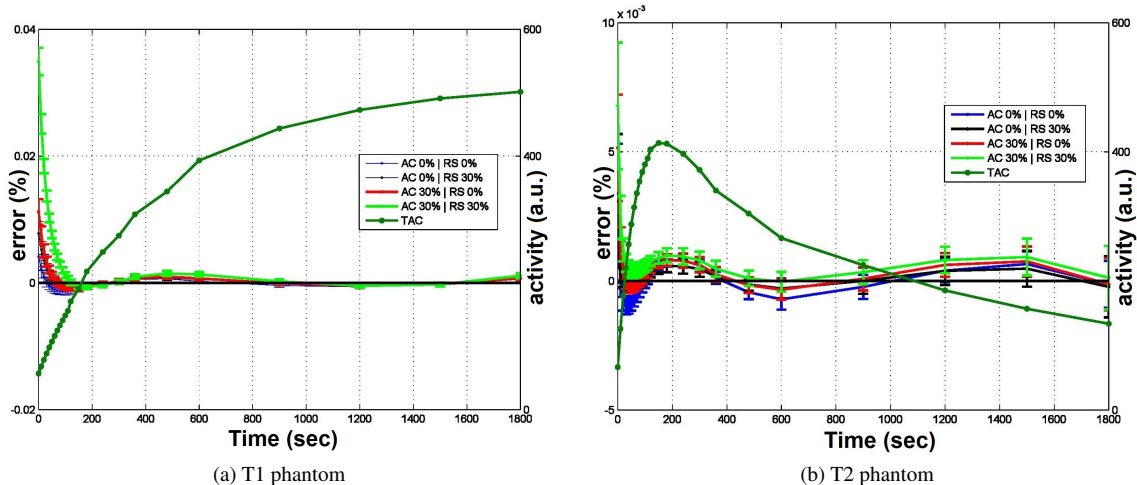


Fig. 3: Dynamic images errors evaluated according to eq.9, with overimposed the relevant TACs.

the tissue is underestimated, also for low noise values.

In the simulation results shown in fig.2(a) and fig.2(b) relevant to tissue T1, the percentage error of the k_4 kinetic parameter seems very high (more than 200%); but it is worth to note that for tissue T1 the input k_4 value (see tab.1) is very low, so in reality the not-normalized error value is very low (less than $1E-4$). As far as all the other k_j parameters in fig.2, the percentage errors are always less than 20%.

The percentage errors of K values for tissue T2 are lower than for tissue T1, as it is evident comparing the curves of fig.2(c) and 2(d) with fig.2(a) and 2(b), respectively; for a better comparison, we used the same scale limits on y-axes in the figures, except for the k_4 parameter. A partial possible reason, that could explain also the less bias observed for the rate constants K_1 and k_2 , can be that T2's kinetic parameters are comparably higher than those of T1 and that the estimation method could be influenced by such a difference in magnitude. Moreover, in T2, the rate constant of k_4 is not negligible as compared to other rate constants. For that reason the influx rate of K_i can not be considered a good parameter of interest for the kinetics, since it assumes an irreversible tracer kinetics with $k_4 = 0$ (we reported it just for sake of completeness).

Regarding the percentage errors on reconstructed images, the results of fig.3 show that the error, as well as depending, as expected, on noise, is higher in low emission images (first points in fig.3(a) and first and last points in fig.3(b)), for any noise percentage values, as it can be seen taking into account the values of the superimposed TAC time series. However, in any case, it is important to note that the percentage error is always less than $1E^{-2}$.

VI. CONCLUSION

In this paper the behaviour of dynamic PET direct reconstruction algorithm on noisy data has been studied. We performed simulations in order to extract indexes that quantitatively describe the goodness of kinetic parameters estimation and dynamic images reconstruction. The results obtained allow us to affirm that the direct reconstruction algorithm tested grant good performance also in presence of noise on simulated data.

The next step of the work will be to validate this error-quantification algorithm on real phantom/clinical dynamic PET scan. Since in direct algorithms we are dealing with raw sinogram data, we believe that the assessment of the final output of reconstruction and parameter estimation should be evaluated on those data. In fact, the objective of the future work is to define a new method for assessing the error in parameter estimation from the knowledge of the noise that affects measured data.

CONFLICT OF INTEREST

The author confirm that this article content has no conflicts of interest.

ACKNOWLEDGEMENTS

Declared none.

REFERENCES

1. Rowe R W, Dai S. "A pseudo-Poisson noise model for simulation of positron emission tomographic projection data" *Med Phys.* 1992;19(4):1113-9.
2. Kimura Y, Naganawa M et al. "MAP-based kinetic analysis for voxel-by-voxel compartment model estimation: detailed imaging of the cerebral glucose metabolism using FDG" *Neuroimage.* 2006;29(4):1203-11.
3. Santarelli M F, Positano V, Landini L. "Dynamic PET data generation and analysis software tool for evaluating the SNR dependence on kinetic parameters estimation" *IFMBE Proceedings.* 2014;45(4):204-7.
4. Tsoumpas C, Turkheimer F E, Thielemans K. "A survey of approaches for direct parametric image reconstruction in emission tomography" *Med Phys.* 2008;35(9):3963-71.
5. Zhu W, Li Q et al. "Patlak Image Estimation From Dual Time-Point List-Mode PET Data" *IEEE Trans. Med. Imag.* 2014;33(4):913-24.
6. Wang G, Qi J. "An optimization transfer algorithm for nonlinear parametric image reconstruction from dynamic PET data" *IEEE Trans. Med. Imag.* 2012;31:1977-88.
7. Yavuz M, Fessler J A. "Statistical Tomographic Recon methods for randoms precorrected PET scans" *Medical Imaging Analysis.* 1998;2:369-78.
8. Ahn S, Fessler J A. "Emission Image Reconstruction for Randoms-Precorrected PET Allowing Negative Sinogram Values" *IEEE Transactions on Medical Imaging.* 2004;23(5):591-601.
9. Schmidt K C, Turkheimer F E. "Kinetic modeling in positron emission tomography" *Journal of Nuclear Medicine.* 2002;46(1):70-85.

Author: Michele Scipioni
Institute: Fondazione G. Monasterio, CNR-Regione Toscana
Street: via Moruzzi, 1, 56124
City: Pisa (PI)
Country: Italy
Email: michele.scipioni@ing.unipi.it